On the Secondary Instability of Rayleigh-Bénard Convection

Aaron Wienkers

1 Introduction

The Rayleigh-Bénard instability of a thin fluid layer heated from below is a classic example of linear fluid dynamical instability. First observed in experiments by Bénard in 1900, and theorised by Lord Rayleigh later in 1916 for the case of stress-free boundaries, the onset of the instability results in exponential growth of horizontal convection cells, but whose linear growth is quickly saturated by nonlinearities. What Bénard would have most certainly also observed in his experiments is the *secondary* instability of this convection cell state brought about by the first instability. Since the early 1900's, there has been much interest in using these ideas to describe natural phenomena ranging from closed-cell cloud formations, to solar convection cells, and even convection in the Earth's mantle. By the end of the industrial revolution, engineers even became interested in these convective instabilities to exploit the possibly enhanced heat transfer ability.

Although today, the trove of secondary instabilities and further the buoyant turbulence it may educe has been well-characterised, the canonical pattern forming order parameter equations inspired by the instability still entertain mathematicians and physicists alike. This paper will begin by developing the primary and secondary linear instability theory for an infinite Prandtl number fluid, which will then be solved numerically in order to probe the properties of the cross-roll instability. With insight from that investigation, the derivation of the Swift-Hohenberg model parameter equation will be motivated and further used to explore the mesoscale pattern forming ability of this classic nonlinear model.

2 Theoretical Model

2.1 Governing Equations

In variables nondimensionalised using the cavity height, d, and thermal diffusion (κ) timescale, the Boussinesq set is

$$\begin{aligned} \frac{\partial \mathbf{u}}{\partial t} + (\mathbf{u}\cdot\nabla)\mathbf{u} &= \mathrm{Pr}\left(-\nabla\Pi + \theta\hat{\mathbf{z}} + \nabla^2\mathbf{u}\right) \\ \frac{\partial \theta}{\partial t} + (\mathbf{u}\cdot\nabla)\theta &= \mathrm{Ra}\ \mathbf{u}\cdot\hat{\mathbf{z}} + \nabla^2\theta \\ \nabla\cdot\mathbf{u} &= 0 \end{aligned} \tag{1}$$

where θ is the nondimensional temperature anomaly from the quiescent thermal conduction profile. The typical definitions for Rayleigh and Prandtl number are used — $\mathrm{Ra} \equiv \gamma g \Delta T d^3/(\nu\kappa)$, and $\mathrm{Pr} \equiv \nu/\kappa$, where γ is the thermal expansion coefficient, and the conventional variables for each of the other terms are used. When written in this way, the primary basic state is just the trivial solution.

To make this a tractable numerical problem, for the time being $\mathrm{Pr} \to \infty$ will be assumed. Then embedding continuity by a Helmholtz transform into the Poloidal-Toroidal coordinates,

$$\begin{aligned} \mathbf{v}_P &= \nabla \times (\nabla \times \phi \hat{\mathbf{z}}) \\ \mathbf{v}_T &= \nabla \times \psi \hat{\mathbf{z}}, \end{aligned} \tag{2}$$

the reduced set of equations may be written as

$$\begin{aligned} \nabla^4 \nabla_\perp^2 \phi - \nabla_\perp^2 \theta &= 0 \\ \nabla^2 \nabla_\perp^2 \psi &= 0 \\ \frac{\partial \theta}{\partial t} + \left[(\nabla \times (\nabla \times \phi \hat{\mathbf{z}}) + \nabla \times \psi \hat{\mathbf{z}}) \cdot \nabla \right] \theta &= \nabla^2 \theta - \mathrm{Ra} \nabla_\perp^2 \phi \end{aligned} \tag{3}$$

where $\nabla_\perp^2$ is the horizontal Laplacian. The transformed boundary conditions at $z = \pm 1/2$ are then

$$\theta = \phi = \partial_{zz}\phi = \partial_z \psi = 0 \tag{4}$$

The full development of the transformed governing equations and approximation can be found in the handwritten appendix.

2.2 Secondary Basic State

Now for $\mathrm{Ra} > (\pi^2 + \alpha^2)^3/\alpha^2$, it is a well-known result that the quiescent primary basic state is unstable to forming 2D convection rolls. The steady state 2D roll solution with $\hat{y}$-wavenumber α must now be found so that the linear secondary stability problem may be formulated. As detailed in the appendix, a Galerkin expansion in trial functions

$$\theta = \sum_{m,n} a_{mn} \sin\left(n\pi \left(z + 1/2\right)\right) \cos\left(m\alpha y\right) \tag{5}$$

will be used, which automatically satisfy the boundary conditions. Along with the result shown by Chandrasekhar [1961] that the 2D convection rolls have no toroidal flow (i.e. $\psi = 0$), the system (3) can be written concisely as the nonlinear algebraic system,

$$\mathbf{I}_{rpmn} a^{mn} + \mathbf{A}_{rpmnlk} a^{mn} a^{lk} = 0. \tag{6}$$

The elements of the 2-tensor, $\mathbf{I}_{rpmn}$, and 3-tensor, $\mathbf{A}_{rpmnlk}$, are again detailed in the appendix for the interested reader to delve into. This nonlinear system may be solved by Newton-Raphson iterations, and with some care of the choice of the initial guess, will avoid converging to the trivial solution.

2.3 Linearised Stability Problem

The governing equations (3) may now be linearised about the secondary base state, $\tilde{\theta}$ and $\tilde{\phi}$, by writing

$$\theta = \bar{\theta}(y, z) + \epsilon \tilde{\theta}(x, y, z, t) \tag{7}$$

and again noting the simple relation between ϕ and θ coefficients offered by (3.1). The reduced linearised system developed in the appendix is

$$\begin{aligned} \frac{\partial \tilde{\theta}}{\partial t} + \partial_{yz}\bar{\phi}\partial_y\tilde{\theta} + \partial_{yz}\tilde{\phi}\partial_y\bar{\theta} + \partial_{xx}\tilde{\phi}\partial_z\bar{\theta} + \partial_{yy}\bar{\phi}\partial_z\tilde{\theta} + \partial_{yy}\tilde{\phi}\partial_z\bar{\theta} \\ = (\partial_{xx} + \partial_{yy} + \partial_{zz})\tilde{\theta} - \mathrm{Ra}(\partial_{xx} + \partial_{yy})\tilde{\phi}. \end{aligned} \tag{8}$$

The normal Floquet modes look like

$$\tilde{\theta} = e^{\mathrm{i}\mathbf{k}\cdot\mathbf{x}+\sigma t} \sum_{m,n} b_{mn} \left(n\pi \left(z + 1/2\right)\right) e^{m\alpha y}, \tag{9}$$

but following Bolton and Busse [1985], for Pr $\to \infty$, the Floquet coefficient may be ignored, and so the disturbances may be split into a symmetric and antisymmetric component. Multiplying by normal mode (r, p), and integrating over the domain, system (8) can similarly be reduced to the linear algebraic generalised eigenvalue problem,

$$\check{\hat{\tilde{\mathbf{I}}}}_{rpmn} \check{\hat{b}}^{mn} + \check{\hat{\tilde{\mathbf{A}}}}_{rpmnlk} a^{lk} \check{\hat{b}}^{mn} = -c_{rp} \check{\hat{\sigma}}, \tag{10}$$

where $\hat{b}$ corresponds to the symmetric eigencoefficient and $\check{b}$ the antisymmetric eigencoefficient. Again, the elements of these matrices will not be reproduced here, but are derived in the handwritten appendix.

Solution of the generalised eigenvalue problem (10) results in a dispersion relation,

$$\sigma = \sigma(\alpha, \mathrm{Ra}, k_x), \tag{11}$$

for each α and Ra parameterising the base state, and k_x parameterising the perturbations of the secondary instability. This σ is actually the maximum of the anti- and symmetric growth rates. To assess the stability of the 2D convection rolls of a particular α with heating given by Ra, we must find the maximum growth rate over all possible perturbations k_x:

$$\sigma(\alpha, \mathrm{Ra}) = \max_{\forall k_x} \sigma(\alpha, \mathrm{Ra}, k_x). \tag{12}$$

3 Results

3.1 Verification

The nonlinear solver for the secondary basic state was verified against the analytic neutral stability curve for the primary instability, $\mathrm{Ra} = (\pi^2 + \alpha^2)^3/\alpha^2$. For $\mathrm{Ra} \lesssim \mathrm{Ra}_c$, the Newton-Raphson iterations converge to 0 independent of the initial guess. However, for $\mathrm{Ra} \gtrsim \mathrm{Ra}_c$, a nontrivial solution exists, and was compared against the asymptotic solution for small $(\mathrm{Ra} - \mathrm{Ra}_c)$ found by Busse and Bolton [1984].

Similarly, the linear system solution was verified by setting $a^{mn} = 0$, corresponding to the primary stability of the quiescent state. Although this really only confirms that $\tilde{\mathbf{I}}_{rpmn}$ is correct, the validation in the next section will further confirm these results.

3.2 Validation

The numerical results are further validated by directly comparing to the so-called *Busse balloon* in the limit Pr $\to \infty$ [Swinney and Gollub, 1981]. Figure 1 indicates the numerically computed stability of the secondary base state, next to the Busse balloon recreated by Schnaubelt and Busse [1989]. Unfortunately, due to the nonlinearity in computing the basic state, this problem scales as $\mathcal{O}(N^6)$. Thus, only $N = 8$ modes in the y and z directions could reasonably be used to solve the stability problem. For $\mathrm{Ra} < 5 \cdot 10^3$, $N = 8$ modes produces a well-converged solution; however, with increasing Ra, increasingly more modes are required. At $\mathrm{Ra} = 5 \cdot 10^4$, $N = 14$ modes were necessary to gain reasonable convergence, and so no higher Ra were explored. Schnaubelt and Busse [1989] themselves admit and show that their numerics are not converged for very large Ra.

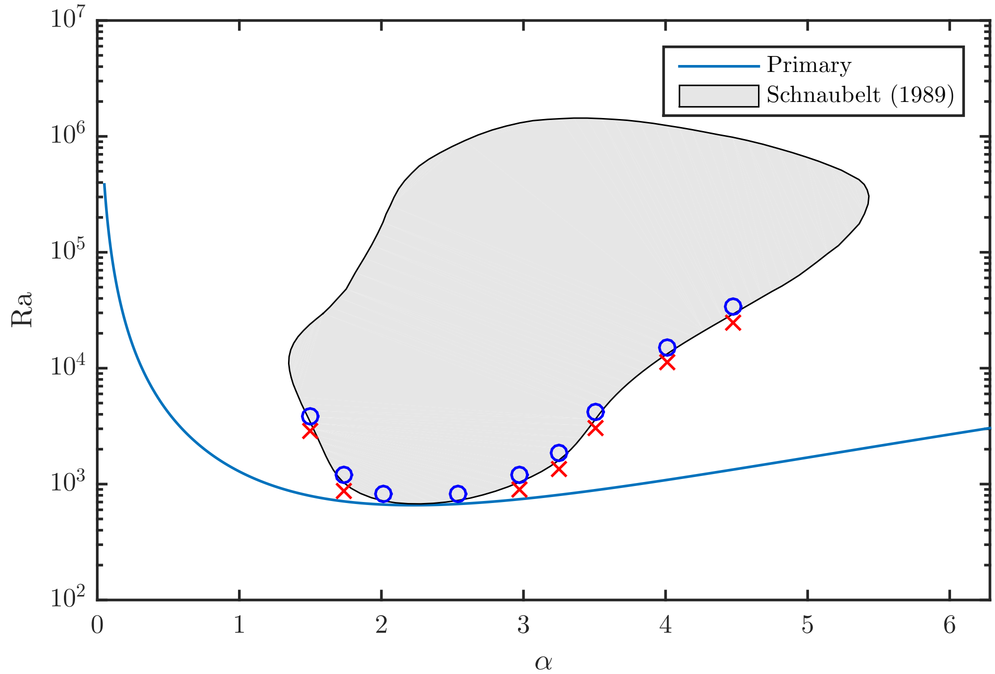

Figure 1: Validation against the Pr $\to \infty$ limit of the Busse balloon Schnaubelt and Busse [1989]. Red $\times$'s mark the numerical solutions with a positive eigenvalue, and $\circ$'s mark solutions with stable secondary basic states.

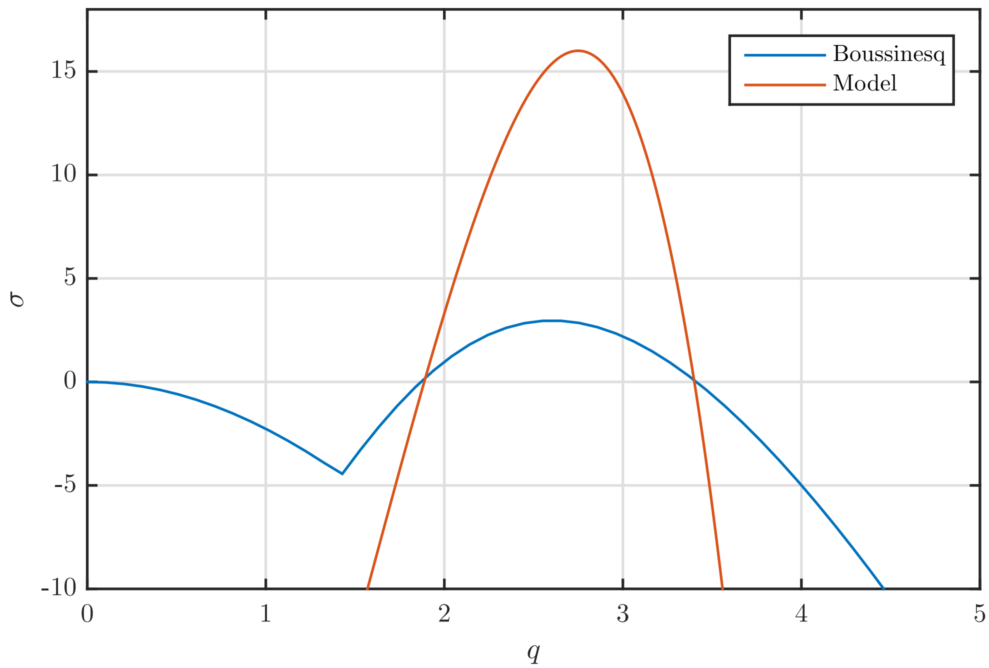

Figure 2: Growth rate, σ, shown over a range of wavenumbers, motivating the construction of the order parameter equation linear growth function, modelled here for an example case with $\mathrm{Ra} = 6000$ and $\alpha = 4$.

3.3 Order Parameter Equation Model

Looking at the eigenvalue solution of (10) as a function of the perturbation wavenumber, k_x, shows some generic behaviour which we can exploit to motivate an order parameter model. A typical plot of growth rate vs k_x is shown in Figure 2, which notably shows that there is a range of k_x that the 2D convection rolls (with α) are unstable to. Moreover, Ra only appears to act to shift $\sigma(k_x)$ up or down, either increasing or decreasing the overall stability. The simplest polynomial model which captures the desired functional behaviour of the dispersion relation with respect to the model wavenumber, q, is

$$\sigma(q) = \mu - (q_c^2 - q^2)^2 \tag{13}$$

where the forcing term, μ, destabilising this system is $\propto$ Ra. If desired, time can be scaled here to match the magnitude of the growth rate in the physical system, but we need only care about the sign of σ for the purposes of this model.

For 3D perturbations of the form

$$\phi \propto e^{\sigma t} e^{\mathbf{i}\mathbf{q}\cdot\mathbf{x}}, \tag{14}$$

a sort of reverse normal mode analysis can be conducted. Thus the PDE which produces these desired linear stability characteristics is

$$\partial_t \phi = \left[\mu - (q_c^2 + \nabla^2)^2\right] \phi. \tag{15}$$

However, as designed, this PDE will continue exhibiting linear growth for all t. Swift and Hohenberg [1977] proposed to saturate the linear instability by adding a nonlinear term $\propto \phi^3$:

$$\partial_t \phi = \left[\mu - (q_c^2 + \nabla^2)^2\right] \phi - \phi^3. \tag{16}$$

The Swift-Hohenberg equation (16) was evolved in time with a Fourier-Spectral collocation method to demonstrate the utility of this order parameter model, and its ability to capture not only the cross-roll instability but also other finite Pr instabilities. Nonetheless, for brevity, the nonlinear dynamics of the Swift-Hohenberg model will not be further discussed. The interested reader is referred to the authoritative review by Cross and Hohenberg [1993].

4 Conclusion and Learning Points

In this work, I have recreated the timeless results of Busse for infinite Prandtl number, and whose result was first produced in Schnaubelt and Busse [1989]. Initial attempts at a generalised formulation for finite Prandtl number and no-slip boundaries were unfortunately thwarted, initially by the computationally prohibitive mode requirement when solving the nonlinear system using Fourier-Chebyshev trial functions which quite poorly resemble the solution. A second attempt rather using the bases developed by Chandrasekhar [1961] which embeds the no-slip boundary conditions was analytically more complex (solving 32 separate triple trigonometric integrals). Ultimately, this was also foiled when convergence of the nonlinear solver to a nontrivial solution in these bases could not be obtained.

Returning to the simpler case with stress-free boundaries and simpler trial functions, convergence to the basic state was found and the cross-roll instability could finally be characterised. Nonetheless, in the absence of these restrictive assumptions, it has become apparent that for a given basic primary instability, the secondary instabilities are numerous and generally exhibit far richer behaviour. This appears to be — at least in the case of convection — due in part to the breaking of horizontal symmetries and isotropy of the initial basic state by the growth of the primary instability. In many cases, this does not result in such rich deterministic behaviour as described in this paper, but rather immediately becomes chaotic or turbulent.

In the face of such complexity of the nonlinear saturated state, it has become apparent the utility of order parameter equations in giving valuable insight into otherwise complex 3D systems. Although it appears to be more of an art than a science (e.g. using a cubic nonlinearity versus quadratic or quartic), this family of model equations sheds light on a powerful method of generating reduced models which still captures the stability and saturation characteristics of the physical system. Therefore, they are likely to see future utility in understanding chaotic or weakly turbulent fluid systems.

References

E. W. Bolton and F. H. Busse. Stability of convection rolls in a layer with stress-free boundaries. *Journal of Fluid Mechanics*, 150:487–498, 1985.

F. H. Busse and E. W. Bolton. Instability of convection rolls with stress-free boundaries near threshold. *Journal of Fluid Mechanics (ISSN 0022-1120)*, 146(-1):115–125, Sept. 1984.

S. Chandrasekhar. *Hydrodynamic and hydromagnetic stability.* International Series of Monographs on Physics, 1961.

M. C. Cross and P. C. Hohenberg. Pattern formation outside of equilibrium. *Reviews of Modern Physics*, 65(3):851–1112, July 1993.

M. Schnaubelt and F. H. Busse. On the stability of two-dimensional convection rolls in an infinite Prandtl number fluid with stress-free boundaries. *Zeitschrift für Angewandte Mathematik und Physik. ZAMP. Journal of Applied Mathematics and Physics. Journal de Mathématiques et de Physique Appliquées*, 40(2):153–162, 1989.

J. Swift and P. C. Hohenberg. Hydrodynamic fluctuations at the convective instability. *Physical Review A*, 15(1):319–328, Jan. 1977.

H. L. Swinney and J. P. Gollub, editors. *Hydrodynamic Instabilities and the Transition to Turbulence*, volume 45 of *Topics in Applied Physics.* Springer Berlin Heidelberg, Berlin, Heidelberg, 1981.